

Robust Federated Learning in the Face of Covariate Shift: A Magnitude Pruning with Hybrid Regularization Framework for Enhanced Model Aggregation

Özgü Göksu
School of Computing Science
University of Glasgow
2718886G@student.gla.ac.uk

Nicolas Pugeault
School of Computing Science
University of Glasgow
nicolas.pugeault@glasgow.ac.uk

Abstract—The development of highly sophisticated neural networks has allowed for fast progress in every field of computer vision, however, applications where annotated data is prohibited due to privacy or security concerns remain challenging. Federated Learning (FL) offers a promising framework for individuals aiming to collaboratively develop a shared model while preserving data privacy. Nevertheless, our findings reveal that variations in data distribution among clients can profoundly affect FL methodologies, primarily due to instabilities in the aggregation process. We also propose a novel FL framework to mitigate the adverse effects of covariate shifts among federated clients by combining individual parameter pruning and regularization techniques to improve the robustness of individual clients’ models to aggregate. Each client’s model is optimized through magnitude-based pruning and the addition of dropout and noise injection layers to build more resilient decision pathways in the networks and improve the robustness of the model’s parameter aggregation step. The proposed framework is capable of extracting robust representations even in the presence of very large covariate shifts among client data distributions and in the federation of a small number of clients. Empirical findings substantiate the effectiveness of our proposed methodology across common benchmark datasets, including CIFAR10, MNIST, SVHN, and Fashion MNIST. Furthermore, we introduce the CelebA-Gender dataset, specifically designed to evaluate performance on a more realistic domain. The proposed method is capable of extracting robust representations even in the presence of both high and low covariate shifts among client data distributions.

I. INTRODUCTION

Federated learning (FL) provides an efficient solution for multiple users to train a joint, common model while preserving the privacy of their data. This data privacy is crucial for a wide range of applications, where the user data can be valuable or sensitive.

In a typical FL framework, a centralized global model broadcasts across multiple clients, with each client training its copy of the model independently on its local dataset. The model parameters are then aggregated to update the global model [14], [17]. In the ideal case, the global model will provide better accuracy and generalisation than local models trained on smaller, partial datasets could achieve. A fundamental assumption in this process is that the local models

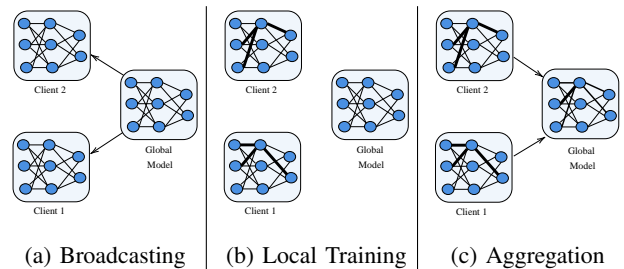


Fig. 1: Illustration of the FedAvg process. The thickness of lines represents the highly relevant, high-impact weights in the client network model. After merging, critical weights are drastically weakened affecting network performance.

can be merged successfully, but data heterogeneity can lead to large divergence in local models’ weights and cause the model aggregation step to be unstable and challenging (see Fig. 1). This is a critical issue since it slows convergence, weakens generalization across clients and causes inconsistent model performance systems [19].

This issue can be particularly salient in real-life cases, especially in data scenarios where the number of clients is limited, yet data heterogeneity is significantly high. For example, consider a small number of specialised imaging laboratories across the world: in that case, the number of nodes is likely to be relatively small, each node is likely to hold a relatively small dataset, and the distribution of cases is likely to vary widely between sites. This article demonstrates experimentally that most FL approaches see a large drop in performance when clients are trained with data with large inter-client differences in distribution, even approaches that perform well on small covariate shifts.

We argue that this performance drop is essentially caused by the inefficiency of merging networks with divergent weights. We propose a novel framework, FEDMPR (Federated Learning Magnitude Pruning with Regularization) to improve FL in scenarios with large data heterogeneity by training local net-

works that are more robust to the merging step, using a combination of three process: Magnitude-based pruning to remove unnecessary parameters, dropout to encourage redundancy in neural decision pathways, and noise injection to improve robustness of networks outputs to small weight variations. We demonstrate that this framework outperforms standard FL approaches on all benchmarks, in particular in datasets with large covariate shifts between clients. Additionally, we introduce a novel dataset for heterogeneous FL, called CelebA-gender. This dataset, drawn from the CelebA face dataset [12], is specifically designed to evaluate the performance of FL methods in challenging data distribution scenarios, where the distribution difference between clients is not caused merely by class imbalance, but by within-class distribution differences. By addressing the shortcomings of current FL approaches, our framework aims to advance the state-of-the-art in FL and enable more effective deployment in real-world applications. Our framework presents several key contributions:

- **FEDMPR:** we propose a new framework for robust Federated Learning in scenarios with high-covariate shifts between clients data.
- **Data Heterogeneity Scenarios:** our methodology provides several levels of data heterogeneity among many clients to evaluate the adaptability of federated learning approaches.
- **Novel Classification Dataset:** we present a reconstructed gender classification dataset based on attributes to enable a thorough evaluation of our framework and comparison with existing approaches.

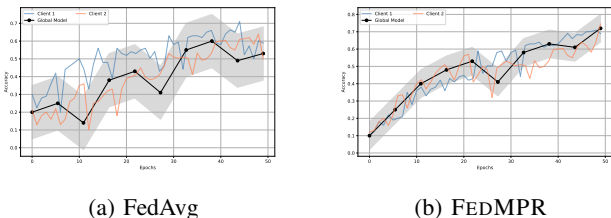


Fig. 2: Training process of FL with two nodes: 2a FedAvg shows clear drops in performance at each merging step, due to the volatility of the merging process; 2b the FEDMPR framework reduces the negative effect of merging models and achieves better performance (training with two nodes on CIFAR10).

II. BACKGROUND

Federated Parameter Selection

Federated learning (FL) approaches encounter several critical challenges, particularly poor convergence on highly heterogeneous data and the lack of solutions for individual clients. To address these issues, parameter selection or decoupling FL approaches introduce tailored models for heterogeneity [16], [19], [20]. Among these approaches, some studies [16], [19] manually partition the model into personalized and shared parameters. Personalized methods can

address the data heterogeneity. When clients have imbalanced, or highly distributed data, these algorithms cannot learn robust features. However, a core question remains unresolved: how we can effectively eliminate redundant parameters in local models, especially when there are relatively few clients and substantial data heterogeneity among them without personalized.

Data Heterogeneity in Federated Learning Numerous algorithmic solutions have been proposed in the literature to address the challenges posed by data heterogeneity in federated learning [13], [2]. These approaches often introduce proximal terms to constrain local updates concerning the global model, aiming to mitigate the adverse effects of client data diversity. While these approaches reduce the divergence between local and global models, they simultaneously hinder local convergence, thereby diminishing the amount of information gained in each communication round. Unfortunately, many existing FL algorithms fail to consistently cause stable performance improvements across diverse non-i.i.d. (non-independent and identically distributed) scenarios, when compared to traditional baselines [11], [14], [4], especially in vision tasks such as classification of genders or emotions. For instance, FedBABU [16] addresses data heterogeneity by updating only the model’s body parameters while keeping the head randomly initialized and fixed during local training, sharing only the body with the central server. However, a significant gap remains in effectively addressing data heterogeneity, particularly in cases where covariate shifts among clients are more substantial.

Regularization in Federated Learning

FedProx[17] introduces a proximal term in the loss function that regularizes the local model updates. This regularization term limits the local updates from diverging too far from the global model, addressing issues such as the partial participation of clients in FL. SCAFFOLD [7] introduces a control variate-based regularization method to correct for client covariate shifts in non-i.i.d. The work [10] estimates weight distribution regularization for each client using the FedAvg. Consequently, the regularization based FL approaches may suffer from real-world applications where the classes are completely different per client, leading to instability in distribution estimation.

III. FEDERATED LEARNING FOR SMALL NUMBER OF LARGE NON-IID CLIENTS

A. Federated Learning

Federated Learning (FL) is a decentralized approach to machine learning that allows multiple clients (e.g., mobile devices, sensors, organizations) to train a global model collaboratively while keeping their local data private. Federated learning frameworks like FedAvg, typically consist of three key steps: broadcasting, local training, and model aggregation into a global model (Figure 1). The central server distributes the current global model to all participating clients after

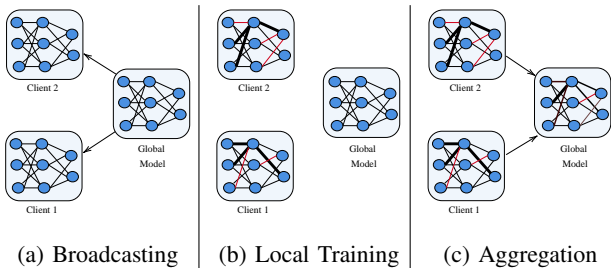


Fig. 3: FEDMPR: The red lines indicate connections that have smaller impact weights. The thickness of lines visually emphasises the weight’s magnitude, with thicker lines signifying more effect. The evaluation plot shows accuracy for clients and the global model, and black dots represent the model aggregation step for the global model.

each merging step (Broadcasting). Each client trains its local copy of the global model with its own private data (Local Training) while data privacy is preserved since the data is never transferred between clients or the server. After local training is completed (or after a set number of epochs), each client provides their local updated model to the central server. The server then aggregates the locally updated models into a new global model (Model Aggregation), that is then broadcasted again in the next round of learning .

Following the typical FL, the data D is distributed across K clients. Let D_k be the local dataset at client k , with $n_k = |D_k|$ denoting the number of data points at client k . The global objective function in FL is then a weighted average of the local objectives:

$$\min_w F(w) = \sum_{k=1}^K \frac{n_k}{n} F_k(w), \quad (1)$$

where $n = \sum_{k=1}^K n_k$ is the total number of data points across all clients and $F_k(w)$ is the local objective function at a client k :

$$F_k(w) = \frac{1}{n_k} \sum_{i \in \mathcal{D}_k} f_i(w). \quad (2)$$

Current research predominantly relies on FedAvg-based model aggregation and training procedures. However, despite similarities between client datasets, individual clients may not learn the same underlying patterns. Large differences in network weights can weaken or break essential decision pathways (see Figure 1) harming the performance of the global model. Furthermore, the broadcasting stage following model aggregation overwrites previously learnt parameters, which might result in slower and poorer convergence. This is visible in Figure 2a where the accuracy of local models is severely affected by each aggregation/broadcasting stage.

B. The Problem of Non-IID Data

Data heterogeneity is challenging in federated learning. FL approaches, such as FedAvg, shown in figure 1, assume all

local models are trained on independent and identically distributed (i.i.d) data, so that the local networks only diverge to a minor extent during training, allowing successful averaging of the network parameters across clients. While FL frameworks can be beneficial for training models without sharing data, they might suffer when the underlying data distributions diverge significantly. When the data distributions vary significantly across clients (ie, non-i.i.d), it can lead to large divergence in network weights during training, and large loss in accuracy during aggregation.

This raises the question of how we can effectively address situations where each client possesses very different subsets of the overall data distribution. In this study, we categorize scenarios as low and high covariate shifts among clients. We define as *high covariate shift* scenarios where each client trains on a subset of the target classes unseen by the other clients. Conversely, a *low covariate shift* occurs when there is an overlap between classes, but not samples. While basic benchmark datasets in the literature focus on class imbalance as the source of non-i.i.d. between nodes, real-world scenarios can also feature within-class distributional differences. To address this, we introduce a novel dataset, CelebA-Gender, for federated gender classification. In this dataset, the high covariate shift condition is achieved by ensuring that distribution of various facial attributes are distinct, while keeping the class balance between male and female constant.

C. The Problem of Federated Model Aggregation

Since FL models cannot directly access the data, aggregating client parameters is a crucial step for learning. This is particularly important in non-i.i.d., where each client may have different data characteristics. In the FedAvg procedure, weights are averaged and broadcast to the clients (Figure 1). However, clients repeatedly experience slow convergence after broadcasting their weights when there is a class imbalance or diverse data distribution (Figure 2a). In contrast, our proposed method, as illustrated in Figure 3, individually trains each client model and eliminates redundant parameters, thereby reducing the impact of updated parameters on local training and global model aggregation, leading to better convergence (Figure 2b).

IV. METHODOLOGY

In order to improve FL robustness to non-i.i.d. cases, PFL approaches have shown that personalizing specific layers can be an effective approach [1], but do not produce a single global model. In contrast, in this work we argue that local overfitting and aggregation issues can both be overcome by modifying the local training of the clients to ensure that the local networks are robust the aggregation operation. In practice, we propose to do this based on three propositions:

- Small weights add noise to the aggregation, and can be eliminated by pruning.
- redundancy in local networks’ decision pathways improves their resilience to aggregation, and can be achieved by applying dropout during training.

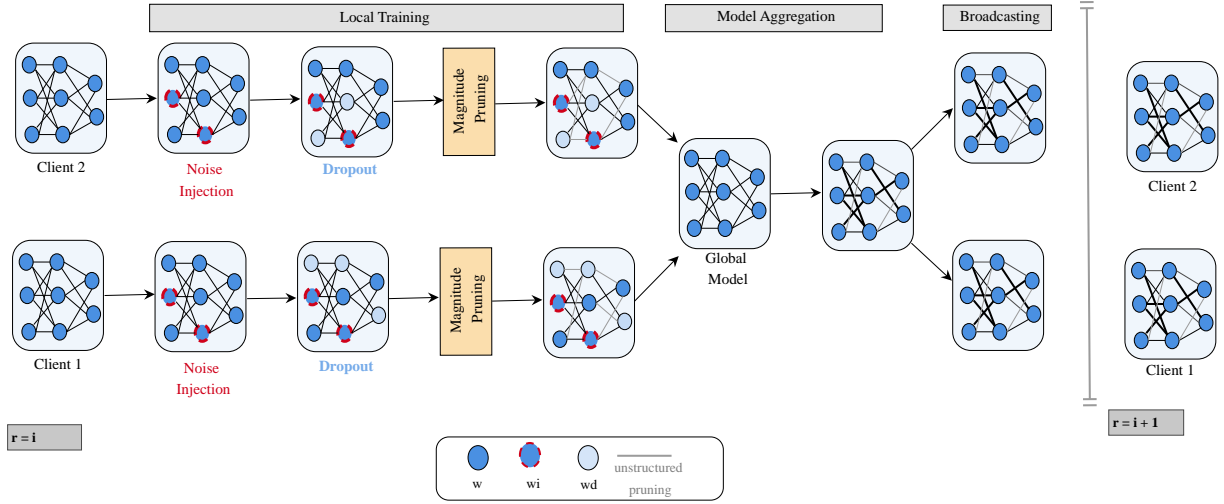


Fig. 4: In the FEDMPR framework, each client employs its regularization method, which integrates dropout during forward propagation and noise injection within each basic block to mitigate local overfitting. The process begins at the i th step with the broadcasting of weights from the central server (global model) to each client, followed by local training and model aggregation. Here, w denotes the unchanged weights during training, w_i represents the weights with Gaussian noise injected, and w_d indicates zeroed weights. Unstructured pruning allows shared weights to be compatible with both the global model and the individual clients.

- Lower sensitivity to individual weights can be achieved by injecting weight noise during training.

We show that the combination of those three improvements enhances performance in model aggregation under both low and high covariate shifts.

A. Pruning

Iterative magnitude pruning (IMP) [3] is introduced to preserve model performance while reducing complexity. The intuition behind network pruning is that weights with smaller values contribute less to the network’s output, and thus, can be removed with minimal impact on the model’s overall performance. IMP’s gradual pruning is less dependent on specific early training conditions, making it more robust across different tasks and architectures. IMP may be more suitable in FL where clients have limited computational resources or the data is highly heterogeneous. When client data distributions differ significantly, the same model can cause weak generalization and destroy the learned features at model aggregation. The problem of “feature destruction” during model aggregation may be explained by averaging weights from models trained on different data distributions. When the weights for specific characteristics are averaged, the outcome of the model may lose the features required to perform successfully on any of the clients’ data. The integration of these methods creates a robust FL framework capable of handling feature destruction, and various data distribution scenarios; ranging from normally distributed data to completely skewed datasets. Our approach presents several advantages, including the prevention of local overfitting, adaptability of client models, and enhanced generalization across diverse datasets, whether they are small,

large, complex, or basic. Here we present the pseudocode of magnitude pruning with FL,

Algorithm 1 Pseudocode of Magnitude Pruning for Layers

Require:

- 1: Central Model c_s ,
- 2: Clients $C = \{c_1, \dots, c_k\}$
- 3: Prune percentage p ,
- 4: Number of rounds R , Number of epochs E
- 5: Training data $D_t = \{d_1, \dots, d_k\}$,
- 6: Validation data D_v

Ensure: Pruned model M

- 7: **for** $i \in [1, R]$ **do**
- 8: $C \leftarrow \text{broadcast}(c_s, D_t)$
- 9: **for** $c_k \in C$ **do**
- 10: $c_k^* \leftarrow \text{train_client}(c_k, d_k, E)$
- 11: $\mathbf{W}_k \leftarrow \text{get_model_weights}(c_k^*)$
- 12: $t \leftarrow \text{per}(|\mathbf{W}_k|, p \times 100)$
- 13: **for** $w_j \in \mathbf{W}_k$ **do**
- 14: **if** $|w_j| < t$ **then**
- 15: $w_j \leftarrow 0.0$
- 16: **end if**
- 17: **end for**
- 18: **end for**
- 19: $\mathbf{c}_s \leftarrow \text{FedAvg}(c_1, \dots, c_k)$
- 20:
- 21: $\text{accuracy}_{\text{server}} \leftarrow \text{evaluate_model}(c_s, D_v)$
- 22: **end for**
- 23: **return** c_s

B. Regularization

Dropout The dropout formula is similarly defined in the paper [18]. During training, for each input x_i to the neuron, the output y_i is modified as follows,

$$y_i = M_i \cdot f(W_i \cdot x_i + b_i) \quad (3)$$

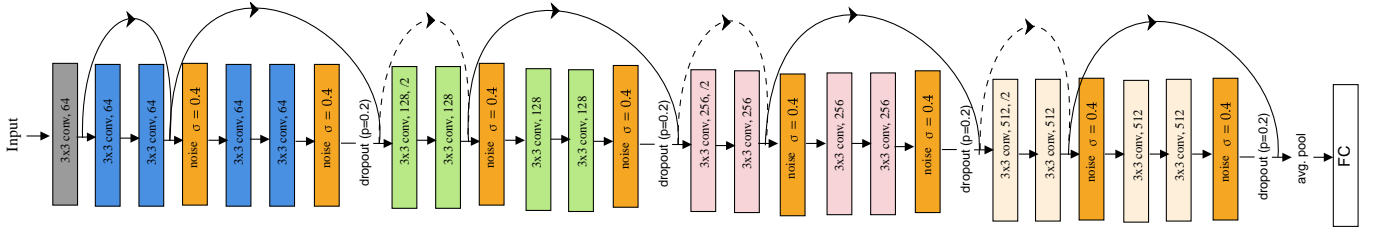


Fig. 5: ResNet-18 model architecture with regularization layers integration.

where W_i and b_i are the weights and biases associated with the neuron, and $f(\cdot)$ is the activation function. The mask M_i lets the neuron's output pass or sets it to zero. The dropout ratio (d) is the likelihood of a specific neurone being deactivated during a forward pass.

Noise Injection is a regularization technique that makes neural networks more robust and less prone to overfitting. In our experiments, the noise injection method encourages the network to avoid over-reliance on specific weights and promotes a more generalized solution. By perturbing the weights slightly during training, the model becomes more robust to small variations in the data and improves its generalization capabilities. We use weight noise injection with Gaussian noise.

Let $W(l)$ represent the weight matrix of a layer l , and let ϵ_W denote the noise added to the weights, where the noise is sampled from a normal distribution $\epsilon_W \sim N(0, \sigma^2)$. The noisy weights are given by

$$W_n(l) = W(l) + \epsilon_W \quad (4)$$

Regularization is incorporated into each local model by introducing randomly generated values specific to each client. This process involves the application of dropout and noise injection within the basic blocks of the network model which is shown in Figure 5, particularly in the early stages of feature extraction. These techniques serve to enhance generalization and robustness by mitigating overfitting and encouraging diverse feature representations during the initial phases of learning.

V. EXPERIMENT

A. High- and Low-covariate shifts datasets

In order to evaluate the effect of covariate-shift on FL, we modify standard datasets in the FL literature (MNIST, FMNIST, CIFAR10 and SVHN) to create different conditions for the clients:

- **Low Covariate Shift** describes a scenario in which the data distributions across individual clients exhibit minimal divergence. For instance, in a two-client setting, the samples from Client 1 closely resemble those from Client 2, ensuring a level of similarity that promotes consistency across data sources. In other words, the client's data distributions are balanced and fully overlap in terms of class labels, yet each client contains unique samples within each shared class. This setup allows for variability in individual data points while maintaining consistency in label representation across clients.

- **High Covariate Shift** describes a scenario in which the data distributions across individual clients display maximal divergence. In a two-client setup on MNIST, CIFAR10, SVHN and Fashion MNIST, one client exclusively trains on samples from classes 0, 1, 2, 3, and 4, while the other client trains on samples from the remaining classes which are 5, 6, 7, 8, and 9. This results in a fully disjoint distribution of samples across clients, with no overlap in class representation, even though each client has a balanced quantity of data within its respective classes.
- **Dirichlet Distribution** This distribution allows for controlled variation in data partitioning, making it highly useful for studying scenarios with heterogeneous client data. α parameter controls the imbalance across clients, smaller α leads to more skewed, non-i.i.d. data partition.

B. CelebA-Gender Dataset

The dataset was constructed from the CelebA dataset, featuring two different scenarios (mutually exclusive and mutually inclusive) and incorporating many specific attributes I . These attributes were selected to ensure balanced data samples for each category, enabling a comparative analysis of low- and high-covariate shift scenarios. We defined two classes, female and male, for the gender classification task. The resulting dataset contains approximately 40,000 images with a resolution of 178×218 , for 3 attributes which are 'Black Hair', 'Smiling', 'High Cheekbones', other attributes are shown in I. We assessed the similarity of the images in each dataset using the FID (Fréchet Inception Distance), where a higher FID score denotes a high covariate shift for clients. To better understand the data distribution among clients, we use a new metric, CLIP embeddings with Maximum Mean Discrepancy (CMMD) [6], to evaluate similarity. Unlike FID, CMMD provides a more effective measure of distribution similarity by leveraging CLIP embeddings and a Gaussian RBF kernel-based mapping for its calculations. CMMD shows the complexity of CelebA-Gender and RAF-DB dataset complexity and other datasets with similar data distributions when there is a low covariate shift in the tableII.

Mutually Exclusive meaning that no sample can simultaneously possess all specified attributes to represent a high covariate shift data distribution. Figure 6, the images from the dataset do not contain a combination of smiling, black hair, and high cheekbones in a single sample. For instance, figure

TABLE I: The list of attributes in CelebA-Gender datasets.

Number of Attributes	Attributes
3	Black Hair, Smiling, High Cheekbones
4	Black Hair, Smiling, High Cheekbones, Mouth Slightly Open
5	Black Hair, Smiling, High Cheekbone, Attractive, Mouth Slightly Open
6	Black Hair, Smiling, High Cheekbone, Attractive, Mouth Slightly Open, Young
7	Black Hair, Smiling, High Cheekbone, Attractive, Mouth Slightly Open, Young, Big Lips

6a depicts a sample that has black hair, no high cheekbones or smiling. Figure 6e shows a sample smiling attribute but no high cheekbones or black hair.

Mutually Inclusive represents situations in which a sample can possess all attributes simultaneously within a single instance, to lead to low covariate shift data distribution, as shown in Figure 7. Image 6c has 3 attributes; smiling, high cheekbones and black hair.



(a) Female (b) Male (c) Male (d) Female (e) Female

Fig. 6: Samples from the CelebA-Gender dataset where the 3 attributes of the samples are mutually exclusive. Each sample in the gender class possesses only one specified attribute at a time.



(a) Female (b) Male (c) Male (d) Female (e) Female

Fig. 7: Samples from the CelebA-Gender dataset where the 3 attributes of the samples are mutually inclusive. Each sample in the gender class possesses three specified attributes at a time.

C. Experimental Setup

Model Our backbone model is ResNet-18. Figure 5 illustrates the ResNet-18 architecture which was manually implemented, we modified the model by reducing the kernel size to 3×3 in the convolutional layers within the basic

blocks. This adjustment was made to suit small-scale datasets such as CIFAR-10 better [8], MNIST [9], Fashion-MNIST [21], and SVHN [15]. For larger and more complex datasets, such as CelebA-Gender the standard kernel size was retained. We report experimental results across a range of benchmark datasets, including CIFAR-10, MNIST, Fashion-MNIST, SVHN and RAF-DB. Additionally, to evaluate performance on more complex data samples, we introduced a novel gender classification dataset, inspired by the CelebA [12] dataset, to further expand the diversity of our evaluation.

Training Setup: the pruning strategy and regularization techniques are uniformly applied across local models, but the weights eliminated during pruning are specific to each local model. Based on our hypothesis, fewer local models exacerbate challenges related to non-i.i.d. and high covariate shifts. Consequently, we selected a client number of 2 to investigate these effects for more cases, also we show the impact of FL on more clients. We employed Stochastic Gradient Descent (SGD) to train each model, with a learning rate of $2e-2$. Each local model was trained for 5 epochs per round. We applied various data augmentation techniques, including random rotation, random flipping, and normalization, to preprocess and enhance the training data.

VI. RESULTS

In Table II, we summarise the performance of state-of-the-art FL algorithms on a range of benchmarks, in the low-covariate shift condition (as evidenced by low FID score between the two clients’ training sets). We also provide the performance of a ResNet18 trained on both clients’ datasets as a baseline, denoted as ‘supervised’. As expected all methods perform well on all datasets in this condition, with lower performance levels on the more complex CIFAR10, CelebA-Gender and the RAF-DB emotion recognition dataset. The results show that pruning based approaches which are FedSelect and FEDMPR can extract robust features from each client data and achieve notably better performance on RAF-DB and CelebA-Gender dataset. FEDMPR achieves best performance on all datasets.

Table III show the same experiment, but with the high-covariate shift condition (as demonstrated by large FID between the clients training sets). We note that accuracy is notably lower on most datasets. FedAvg is particularly affected on CIFAR10, CelebA-Gender and RAF-DB.

Methods that are designed for non-i.i.d. scenarios such as FedSelect perform better across the board, but still achieve low performance on CelebA-Gender. FEDMPR achieves the best performance across the board, with significantly higher performance on CIFAR10 and CelebA-Gender demonstrating the robustness of the approach to high-covariate shift conditions.

In order to evaluate the generality of the results, we report the effect of the clients’ dataset size for the low-covariate shift (Figure 8a) and high-covariate shift (Figure 8b) on CIFAR10. As expected, accuracy increases with larger training sets, and FEDMPR performs best across the board. Additionally, we show the effect of the number of clients in the low-covariate

TABLE II: FL accuracy on low-covariate shift condition (the FID score between the clients’ training sets is low). The reported number is the average test accuracy of the global model over three runs (\pm denotes the standard deviation from the average).

Method	CIFAR10	MNIST	FMNIST	SVHN	CelebA-Gender	RAF-DB
Supervised	91.51	99.08	94.18	93.89	98.39	77.8
FedAvg	77.0 \pm 0.33	99.01 \pm 0.04	90.73 \pm 0.31	91.11 \pm 0.37	91.18 \pm 8.23	43.42 \pm 1.78
FedProx	76.45 \pm 0.89	98.94 \pm 0.16	91.31 \pm 0.54	91.07 \pm 0.17	72.05 \pm 3.86	64.31 \pm 1.45
FedDC	74.37 \pm 2.97	98.58 \pm 0.11	90.04 \pm 0.61	90.44 \pm 0.43	61.67 \pm 7.97	62.43 \pm 1.18
FedDyn	77.72 \pm 0.65	98.98 \pm 0.20	91.13 \pm 1.16	91.57 \pm 0.10	72.07 \pm 4.13	64.39 \pm 1.91
SCAFFOLD	76.73 \pm 0.28	98.77 \pm 0.25	90.87 \pm 0.39	90.97 \pm 0.05	72.13 \pm 4.12	64.51 \pm 1.59
FedSelect	76.25 \pm 1.17	94.91 \pm 2.16	89.78 \pm 2.58	90.32 \pm 1.16	93.14 \pm 3.64	72.74 \pm 1.48
FEDMPR	86.61\pm1.26	99.49\pm0.07	93.1\pm0.46	94.17\pm0.21	96.93\pm 1.05	74.92\pm1.16
FID Score	1.68	0.63	0.83	0.52	12.0	7.79
CMMD Score	0.00	0.00	0.00	0.00	0.02	0.01

TABLE III: FL accuracy in the high-covariate shift condition (the FID between the clients’ training set is high). The reported number is the average test accuracy of the global model over three runs (\pm denotes the standard deviation from the average).

Method	CIFAR10	MNIST	FMNIST	SVHN	CelebA-Gender	RAF-DB
Supervised	91.51	99.08	94.18	93.89	98.39	77.8
FedAvg	51.28 \pm 1.55	89.84 \pm 1.31	80.69 \pm 1.30	75.69 \pm 3.41	47.82 \pm 1.93	45.06 \pm 1.39
FedProx	54.71 \pm 1.25	87.28 \pm 3.04	81.49 \pm 1.18	74.9 \pm 1.21	71.8 \pm 1.92	45.99 \pm 2.84
FedDC	41.09 \pm 1.55	65.62 \pm 9.79	60.11 \pm 6.75	59.02 \pm 2.47	62.77 \pm 6.1	40.55 \pm 0.82
FedDyn	49.48 \pm 0.72	85.53 \pm 2.05	79.33 \pm 2.55	69.71 \pm 2.77	70.5 \pm 3.16	43.12 \pm 1.26
SCAFFOLD	49.18 \pm 0.93	78.73 \pm 5.59	71.06 \pm 3.12	59.09 \pm 2.26	67.63 \pm 7.16	43.11 \pm 1.27
FedSelect	61.97 \pm 5.96	91.02 \pm 4.76	85.01 \pm 5.16	81.00 \pm 4.39	52.5 \pm 4.4	67.45 \pm 4.38
FEDMPR	75.22\pm5.35	98.99\pm0.34	88.92\pm2.24	88.24\pm4.67	84.23\pm1.22	69.41\pm5.54
FID Score	70.69	43.14	47.49	4.52	82.85	9.88
CMMD Score	0.16	0.20	0.10	0.12	1.52	0.17

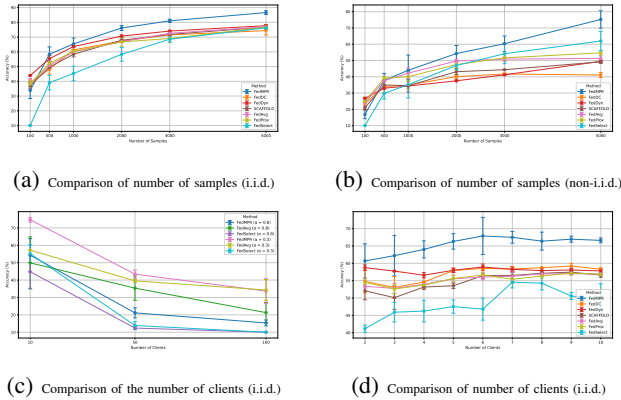


Fig. 8: These plots show the impact of the number of clients and the number of samples per class on federated learning with CIFAR10.

shift version of CIFAR10 in Figures 8c and 8d. In Figure 8d, due to the large number of clients, we used the Dirichlet distribution with parameter $\alpha = 0.3$ for low-covariate shift and $\alpha = 0.8$ for high-covariate shift, to generate the clients’ datasets. When we change the client number from 2 to 10, FEDMPR shows better performance on CIFAR10, FedAvg, and FedProx methods remain stable for client number changes. However, when federating a larger number of clients (50 or 100) we see that the performance of all methods decrease significantly, especially for larger covariate shift (using a Dirichlet distribution with $alpha = 0.8$)

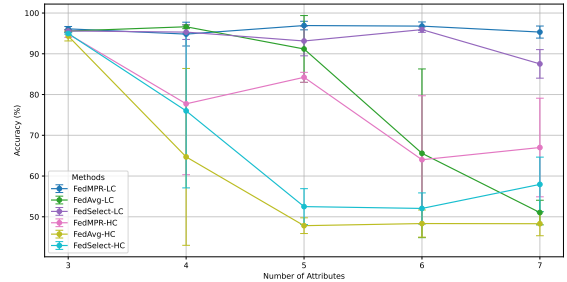


Fig. 9: CelebA-Gender attributes results on several FL methods. HC represents high covariate shift, LC is for low covariate shift.

In Figure 9, we show the impact of the number of attributes selected from Table I on the performance of selected FL algorithms (FedAvg, FedSelect and FEDMPR) in the low- and high-covariate shift conditions. There we see that increasing the number of attributes has little effect in the low-covariate shift condition, as expected, but affects performance in the high-covariate shift condition. We note that FEDMPR shows the best performance in all cases.

VII. ABLATION STUDY

In order to elucidate the respective importance of all the components of the approach, we perform ablation experiments. In our proposed method, there are 3 main parameters: pruning percentage (p), dropout ratio (d) and noise injection percentage

(σ). Pruning percentages, dropout ratios, and noise standard deviations were each examined within a range of 0.2 to 1, and compared to standard FedAvg. Table IV shows the accuracy on the CIFAR10 dataset for low and high covariate shift scenarios.

The pruning has little impact on the low-covariate shift conditions but provides a notable improvement in the high-covariate shift conditions. A small dropout ratio ($d=0.2$) provides a notable improvement in accuracy in both conditions, but larger values (increasing from 0.2 to 0.8) lead to a decrease in performance, especially in the high-covariate shift condition (accuracy decreases from 78.2% to 52.03%). Noise injection lead an increase in performance in both conditions, with the best performance for a higher noise injection of 0.4.

FEDMPR denotes the optimal combination of parameters: a noise injection ratio of 0.4, a dropout ratio of 0.2 and a pruning ratio of 0.4.

TABLE IV: Impact of each component on FL for low- and high-covariate shift conditions on top-1 accuracy on CIFAR10.

Method	Prune	Dropout	Noise	low-CS	high-CS
FL (Baseline)	✗	✗	✗	82.64	72.67
FL ($p=0.2$)	✓	✗	✗	81.84	71.25
FL ($p=0.4$)	✓	✗	✗	81.72	75.63
FL ($d=0.2$)	✗	✓	✗	86.18	78.2
FL ($d=0.8$)	✗	✓	✗	80.36	52.03
FL ($\alpha=0.4$)	✗	✗	✓	84.26	75.76
FL ($\alpha=0.2$)	✗	✗	✓	83.1	74.83
FEDMPR	✓	✓	✓	87.98	80.59

VIII. CONCLUSION

Federated Learning provides an effective solution for the important challenge of allowing multiple clients to train a model jointly, without having to share potentially sensitive data. We have shown that FL can be adversely affected by scenarios where the data distribution between nodes is very different (high-covariate shift condition) due to the volatility of aggregating clients with weights diverging due to training on different data. To address this problem specifically, we proposed a novel FL framework, FEDMPR, that ensures that local clients’ train models that are robust to aggregation, by a combination of weight pruning and regularisation by dropout and noise injection. The experiments confirm the effectiveness of our framework, showcasing a significant performance improvement over existing federated learning methods across multiple benchmark datasets. Moreover, to complement the standard approach in FL to assess distribution differences as class imbalance, we introduced a new dataset, CelebA-Gender, that models within-class distribution differences while keeping class balanced. This dataset is a valuable resource for evaluating and advancing federated learning frameworks in applied settings. Future research will focus on refining pruning mechanisms and exploring more sophisticated regularization techniques to enhance scalability, adaptability, and performance in complex, large-scale federated environments.

REFERENCES

- [1] Liam Collins, Hamed Hassani, Aryan Mokhtari, and Sanjay Shakkottai. Exploiting shared representations for personalized federated learning. In *International conference on machine learning*, pages 2089–2099. PMLR, 2021.
- [2] Yutong Dai, Zeyuan Chen, Junnan Li, Shelby Heinecke, Lichao Sun, and Ran Xu. Tackling data heterogeneity in federated learning with class prototypes. In *Proceedings of the AAAI Conference on Artificial Intelligence*, volume 37, pages 7314–7322, 2023.
- [3] Jonathan Frankle and Michael Carbin. The lottery ticket hypothesis: Finding sparse, trainable neural networks. *International Conference on Learning Representations*, 2019.
- [4] Liang Gao, Huazhu Fu, Li Li, Yingwen Chen, Ming Xu, and Cheng-Zhong Xu. Feddc: Federated learning with non-iid data via local drift decoupling and correction. In *Proceedings of the IEEE/CVF conference on computer vision and pattern recognition*, pages 10112–10121, 2022.
- [5] Darshan Gera and S Balasubramanian. Landmark guidance independent spatio-channel attention and complementary context information based facial expression recognition. *Pattern Recognition Letters*, 145:58–66, 2021.
- [6] Sadeep Jayasumana, Srikumar Ramalingam, Andreas Veit, Daniel Glasner, Ayan Chakrabarti, and Sanjiv Kumar. Rethinking fid: Towards a better evaluation metric for image generation. In *Proceedings of the IEEE/CVF Conference on Computer Vision and Pattern Recognition*, pages 9307–9315, 2024.
- [7] Sai Praneeth Karimireddy, Satyen Kale, Mehryar Mohri, Sashank J Reddi, Sebastian U Stich, and Ananda Theertha Suresh. Scaffold: Stochastic controlled averaging for on-device federated learning. *arXiv preprint arXiv:1910.06378*, 2(6), 2019.
- [8] A Krizhevsky. Learning multiple layers of features from tiny images. *Master’s thesis, University of Tront*, 2009.
- [9] Yann LeCun, Léon Bottou, Yoshua Bengio, and Patrick Haffner. Gradient-based learning applied to document recognition. *Proceedings of the IEEE*, 86(11):2278–2324, 1998.
- [10] Gyuejeong Lee and Daeyoung Choi. Regularizing and aggregating clients with class distribution for personalized federated learning. *arXiv preprint arXiv:2406.07800*, 2024.
- [11] Qinbin Li, Yiqun Diao, Quan Chen, and Bingsheng He. Federated learning on non-iid data silos: An experimental study. In *2022 IEEE 38th international conference on data engineering (ICDE)*, pages 965–978. IEEE, 2022.
- [12] Ziwei Liu, Ping Luo, Xiaogang Wang, and Xiaoou Tang. Deep learning face attributes in the wild. In *Proceedings of the IEEE international conference on computer vision*, pages 3730–3738, 2015.
- [13] Mi Luo, Fei Chen, Dapeng Hu, Yifan Zhang, Jian Liang, and Jiashi Feng. No fear of heterogeneity: Classifier calibration for federated learning with non-iid data. *Advances in Neural Information Processing Systems*, 34:5972–5984, 2021.
- [14] Brendan McMahan, Eider Moore, Daniel Ramage, Seth Hampson, and Blaise Aguera y Arcas. Communication-efficient learning of deep networks from decentralized data. In *Artificial intelligence and statistics*, pages 1273–1282. PMLR, 2017.
- [15] Yuval Netzer, Tao Wang, Adam Coates, Alessandro Bissacco, Baolin Wu, Andrew Y Ng, et al. Reading digits in natural images with unsupervised feature learning. In *NIPS workshop on deep learning and unsupervised feature learning*, page 4. Granada, 2011.
- [16] Jaehoon Oh, Sangmook Kim, and Se-Young Yun. Fedbabu: Towards enhanced representation for federated image classification. *International Conference on Learning Representations*, 2021.
- [17] Pranay Sharma, Rohan Panda, Gauri Joshi, and Pramod Varshney. Federated minimax optimization: Improved convergence analyses and algorithms. In *International Conference on Machine Learning*, pages 19683–19730. PMLR, 2022.
- [18] Nitish Srivastava, Geoffrey Hinton, Alex Krizhevsky, Ilya Sutskever, and Ruslan Salakhutdinov. Dropout: a simple way to prevent neural networks from overfitting. *The journal of machine learning research*, 15(1):1929–1958, 2014.
- [19] Rishub Tamerisa, Chulin Xie, Wenxuan Bao, Andy Zhou, Ron Arel, and Aviv Shamsian. Fedselect: Personalized federated learning with customized selection of parameters for fine-tuning. In *Proceedings of the IEEE/CVF Conference on Computer Vision and Pattern Recognition*, pages 23985–23994, 2024.
- [20] Alysa Ziyang Tan, Han Yu, Lizhen Cui, and Qiang Yang. Towards personalized federated learning. *IEEE transactions on neural networks and learning systems*, 34(12):9587–9603, 2022.

[21] Han Xiao, Kashif Rasul, and Roland Vollgraf. Fashion-mnist: a novel image dataset for benchmarking machine learning algorithms. *arXiv preprint arXiv:1708.07747*, 2017.

IX. APPENDIX

A. Gender Classification

In this study, we introduce the CelebA-Gender dataset, designed to facilitate the evaluation of covariate shift ratios in real-world applications. While existing research predominantly relies on datasets like CIFAR-10, which consists of entirely distinct classes (e.g., deer, cars), these scenarios do not fully capture the complexities of real-world data distributions. Specifically, in the context of facial recognition, the challenge of partitioning data to represent varying degrees of covariate shift remains largely unexplored. Moreover, different facial attributes exhibit distinct behaviours influencing feature learning, further underscoring the need for a dataset tailored to this nuanced setting.

Our proposed dataset addresses these gaps, offering a platform to study and quantify covariate shifts in a realistic and meaningful manner. We begin our analysis with a dataset containing three attributes and progressively expand to a seven-attribute version. The selection of attributes is carefully optimized to maximize the number of samples in each dataset version, ensuring a balance between high-covariate (HC) and low-covariate (LC) conditions. This approach minimizes the risk of overfitting while maintaining balanced data distributions across the different configurations.

Conversely, when the covariate shift among datasets is minimal, the datasets demonstrate higher degrees of similarity, as reflected by lower FID scores. This analysis underscores the impact of covariate shifts on dataset similarity in federated settings. Increasing the number of attributes in cases with high covariate shift reduces the availability of selected samples, as the dataset becomes sparsely populated in the overall data space. This results in a smaller subset of samples that simultaneously satisfy the conditions for all selected attributes. For example, selecting seven attributes narrows the dataset to highly specific samples, and adding more attributes further diminishes this subset. Consequently, we limited the attribute selection to seven attributes, as incorporating a higher number of attributes would yield an insufficient sample size, making it challenging to learn robust and generalizable features effectively.

Table V depicts the FID scores for low and high covariate shifts to measure data distribution. As the number of attributes increases, the complexity of the dataset grows as well, leading to an increasing divergence between the training and test data distributions. For example, the attribute 'Young' oppositely impacts dissimilarity as the 'Attractive' attribute. Table V shows that each attribute has a distinct effect on the similarity of data distributions, implying that attributes cannot uniformly influence distribution.

Figure 10, 11 show the 4 attributes cases. In these images 10, only one attribute is present at a time. For example, the image 10a possesses only the 'High-cheekbones' attribute and

TABLE V: FID score table shows the similarity between attributes when there are low and high covariate shift data distributions. FID scores represent the similarity measurement for the entire datasets and test data. Table VI shows which attributes are added as a new one.

Number of Attributes	3	4	5	6	7
FID (LC)	1.96	6.46	12	13.59	16.79
FID (HC)	65.43	72.71	82.85	77.6	80.92
FID (Train-Test)	5.69	22.41	26.97	26.71	28.65

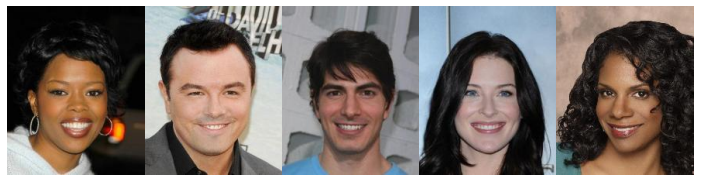
TABLE VI: The list of attributes in CelebA-Gender data.

Number of Attributes	Attributes
3	Black Hair, Smiling, High Cheekbones
4	Black Hair, Smiling, High Cheekbones, Mouth Slightly Open
5	Black Hair, Smiling, High Cheekbone, Attractive, Mouth Slightly Open
6	Black Hair, Smiling, High Cheekbone, Attractive, Mouth Slightly Open, Young
7	Black Hair, Smiling, High Cheekbone, Attractive, Mouth Slightly Open, Young, Big Libs



(a) Female (b) Male (c) Male (d) Female (e) Female

Fig. 10: Samples from the CelebA-Gender dataset where the 4 attributes of the samples are mutually exclusive. Each sample in the gender class possesses only one specified attribute at a time.



(a) Female (b) Male (c) Male (d) Female (e) Female

Fig. 11: Samples from the CelebA-Gender dataset where the 4 attributes of the samples are mutually inclusive. Each sample in the gender class possesses 4 specified attributes at a time.

does not exhibit any other attributes which are 'Black Hair', 'Smiling', or 'Mouth Slightly Open'. Another image 10b has only the 'Mouth Slightly Open' attribute.



(a) Female (b) Male (c) Male (d) Female (e) Female

Fig. 12: Samples from the CelebA-Gender dataset where the 5 attributes of the samples are mutually exclusive. Each sample in the gender class possesses only one specified attribute at a time.

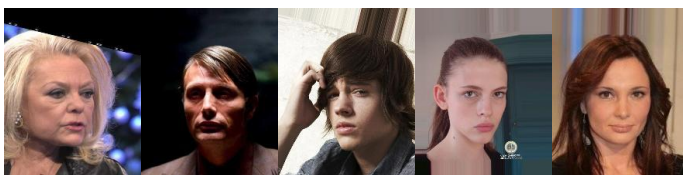
Figure 12, 13 show the 5 attributes for mutual exclusive and inclusive scenarios. In these images 12, only one attribute is present at a time. For example, the male image 12c has only



(a) Female (b) Male (c) Male (d) Female (e) Female

Fig. 13: Samples from the CelebA-Gender dataset where the 5 attributes of the samples are mutually inclusive. Each sample in the gender class possesses 5 specified attributes at a time.

the 'Mouth Slightly Open' attribute and does not exhibit any other attributes which are 'Black Hair', 'Smiling', 'Attractive' or 'High-cheekbones'. Another male image in Figure 13b has all 5 attributes. Figure 14, 15 show the 6 attributes cases. In these images 14, only one attribute is present at a time. For example, the image 14d possesses only the 'Young' attribute and does not exhibit any other attributes which are 'Black Hair', 'Smiling', or 'Mouth Slightly Open', 'Attractive', and 'Mouth Slightly Open'. Another female image 15e presents 6 attributes. Figure 16, 17 show the 7 attributes cases. In these images 17 present 7 attributes at the same time for



(a) Female (b) Male (c) Male (d) Female (e) Female

Fig. 14: Samples from the CelebA-Gender dataset where the 6 attributes of the samples are mutually exclusive. Each sample in the gender class possesses only one specified attribute at a time.



(a) Female (b) Male (c) Male (d) Female (e) Female

Fig. 15: Samples from the CelebA-Gender dataset where the 6 attributes of the samples are mutually inclusive. Each sample in the gender class possesses 6 specified attributes at a time.



(a) Female (b) Male (c) Male (d) Female (e) Female

Fig. 16: Samples from the CelebA-Gender dataset where the 7 attributes of the samples are mutually exclusive. Each sample in the gender class possesses only one specified attribute at a time.

each sample. For example, the image 17b possesses the 'High-cheekbones', 'Black Hair', 'Smiling', 'Mouth Slightly Open', 'Young', 'Attractive' and 'Big Lips'. Another image 16c has only the 'High-cheekbones' attribute. Figure VII shows the performance of gender classification on CelebA-Gender test data. FedDC performs lowest on test data compared to the other approaches. This is because it depends considerably on locally learnt features, leading to it more dependent to the effects of data heterogeneity. When models are aggregated, the locally learnt features may not generalize adequately, resulting in poor classifying of test data. FedMPR, on the other hand, accurately captures representative features that generalize better.

B. Image Classification






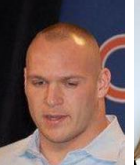















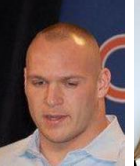







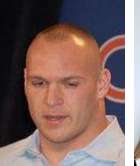







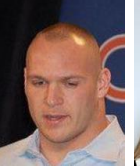







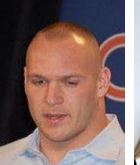







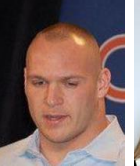







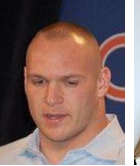


CIFAR-10 consists of 10 classes: airplane, automobile, bird, cat, deer, dog, frog, horse, ship, and truck. To analyze the impact of covariate shift, we define two scenarios: high covariate shift and low covariate shift. The FID score in Figure



(a) Female (b) Male (c) Male (d) Female (e) Female

Fig. 17: Samples from the CelebA-Gender dataset where the 7 attributes of the samples are mutually inclusive. Each sample in the gender class possesses 7 specified attributes at a time.

TABLE VII: Classifier performance on CelebA-Gender test data; green shows correct classification, red represents incorrect.

Method	Images							
Ground Truth								
	Female	Male	Male	Male	Female	Male	Female	Female
FedAvg								
	Male	Male	Male	Female	Male	Male	Female	Female
FedProx								
	Male	Male	Female	Female	Male	Male	Female	Female
FedDC								
	Female	Male	Female	Female	Male	Female	Female	Male
FedDyn								
	Male	Female	Male	Male	Female	Female	Male	Female
SCAFFOLD								
	Male	Female	Female	Male	Female	Female	Male	Female
FedSelect								
	Female	Female	Male	Male	Male	Male	Female	Male
FedMPR								
	Male	Female	Male	Male	Female	Female	Female	Female

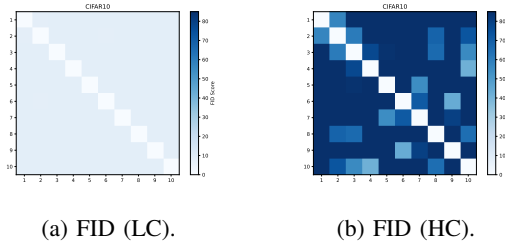


Fig. 18: The impact of attributes on FL methods and the confusion matrices illustrate the discrepancy between 10 clients of CIFAR10 data.

18 is used to quantify the similarity of data distributions across 10 clients in these scenarios.

In the high covariate shift scenario, each client is assigned samples from only one class, leading to highly distinct data distributions between clients. As an alternative, in the low covariate shift scenario, each client has samples from all 10 classes, resulting in more balanced and similar distributions across clients. This comparison highlights how the distribution of class samples influences the overall data similarity in federated learning. Figure 19 illustrates t-SNE plots of different datasets in a low covariate shift scenario. FedAvg demonstrates performance on the MNIST dataset but struggles to learn robust features for more complex datasets such as CIFAR-10 and RAF-DB. Despite having similar data distributions across clients, the FedAvg model aggregation approach based on averaging weights fails to capture robust and discriminative features in these datasets effectively.

C. Emotion Classification

Real-world Affective Faces Database (RAF-DB) is a facial expression dataset with around 30K diverse facial images [5]. It includes 7 classes of basic emotions; Surprised, Fearful, Disgusted, Happy, Sad, and Angry. Each image size is 100×100 and the number of samples for each class is different in an imbalanced dataset. The FID score for the RAF-DB dataset is 7.79 under low covariate shift and 9.88 under a high covariate shift. Notably, the FID scores for data from two clients are relatively high and closely aligned. Figure 20 illustrates the FID scores for each emotion, revealing that the relationships between emotions are complex and inconsistent. This complexity contrasts with the CelebA-Gender dataset, where the data distribution is more straightforward. These findings highlight that emotion classification on RAF-DB presents unique challenges, differing significantly from experiments conducted on datasets like CelebA-Gender.

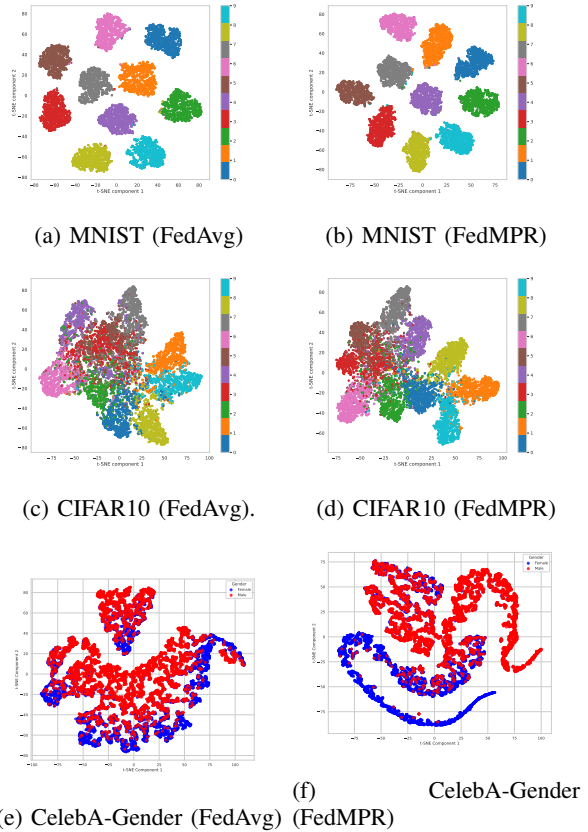


Fig. 19: Data distributions of 3 different datasets in an LC scenario. MNIST contains digits from 0 to 9, and CIFAR10 contains 10 classes such as deer, and horse. CelebA-Gender is a gender classification dataset with 2 classes; Female and Male.

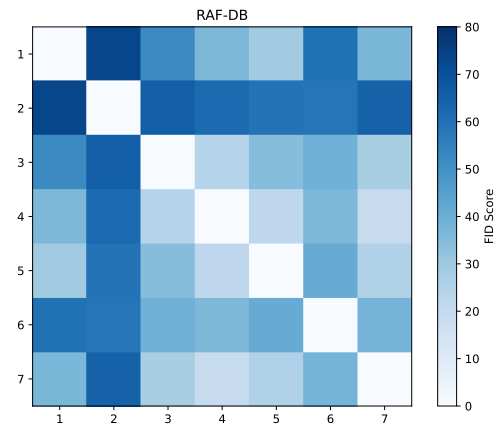


Fig. 20: Emotion classification FID score for each class